DISPLACEMENT-LENGTH SCALING RELATIONSHIPS OF LARGE THRUST FAULTS ON MARS

Corbin L. Kling[1] (corbayn@uga.edu) and Christian Klimczak[1], Structural Geology and Geomechanics Group, Department of Geology, University of Georgia, 210 Field Street, Athens, GA, USA

Summary: We study the topographic expressions of large landforms interpreted to be produced by the accumulation of displacement along lithospheric-scale thrust faults on Mars. Through detailed mapping and analysis of topographic variations along the landforms, the maximum displacements for each of the underlying faults were determined and compared to their respective fault lengths. This data was used to study the statistical relationship between these two parameters. A total of 29 thrust faults from the southern highlands were included in this displacement-to-length analysis.

Introduction: Thrust faults are easily identifiable on planets with little or no erosion due to the distinct morphologies of ridges that result from the accumulation of displacement along the faults [e.g., 1]. The ridges that define the surface expression of thrust faults consist of asymmetric anticlines located near the surface break of the fault and broad synclines trailing off in the direction of the fault dip [2]. Many factors govern the geometry of the ridge, including fault size, fault dip angle, depth of faulting, as well as displacement distribution along the fault plane [1-4]. Topographic data allows for the analysis of these ridges to infer details concerning the geometry and kinematics of the faults, such as the total vertical displacement (i.e., fault throw) that produced the structural relief of the ridge [1]. The distribution of displacement along the lengths of individual faults gives insight into fault growth and overall fault architecture and has implications for lithospheric properties [5, 6].

Study Areas: For our fault displacement analysis, we concentrated on the largest thrust fault-related landforms. A total of 29 individual faults belonging to 6 large fault zones were included in the analysis. The locations of the studied fault zones fell within the southern highlands (Fig. 1), with the exception of one previously analyzed fault zone at Phlegra Montes [7].

Methods: Candidate faults were identified on the Mars Orbiter Laser Altimeter (MOLA) global digital elevation model (DEM) and hillshade (Fig. 1). High Resolution Stereo Camera (HRSC) and Context Camera (CTX) imagery was then used for the detailed mapping of the candidate faults with MOLA only used when imagery was unavailable. After the mapping was complete, the spheroidal lengths of the faults were computed in ArcGIS® using Jennessent's Tools for Graphics and Shapes plug-in [8]. Perpendicular topographic transects were taken in ~ 10 km intervals along the fault traces using MOLA global DEM data. These transects were then plotted and the throw was measured using R Statistical Computing software [9].

Measured throws were then plotted along the fault length to generate a throw profile for each fault studied. If there was more than one fault in a system, the cumulative throw profile was generated by summing the throw of the faults at each point where they overlapped in the system. The maximum measured throw for each fault was then converted into maximum displacement for fault dip angles of 30° ± 5° [1] and paired with the length of that fault. A

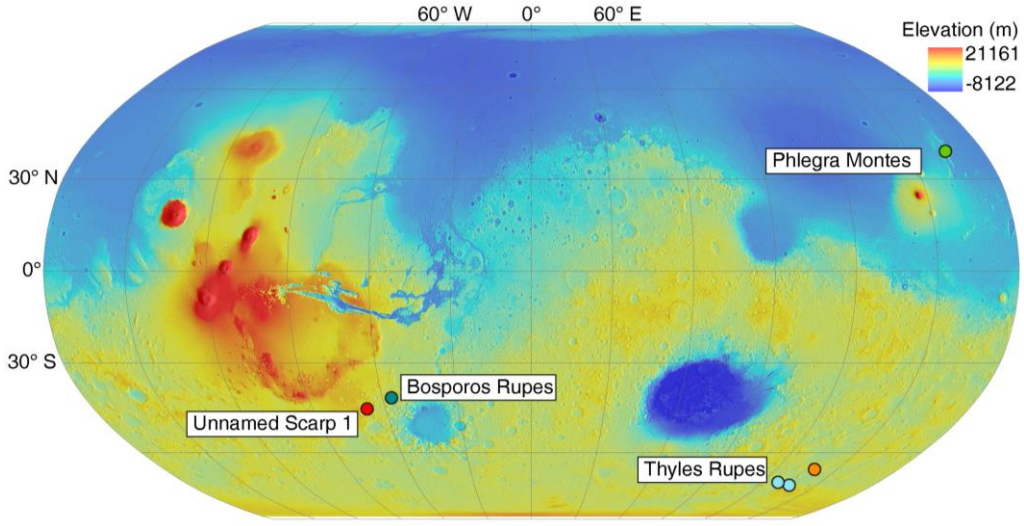

Figure 1) MOLA global DEM overlaid on a MOLA-generated hillshade model with study areas shown as colored dots. Color-coding corresponds to data points in Fig. 2.

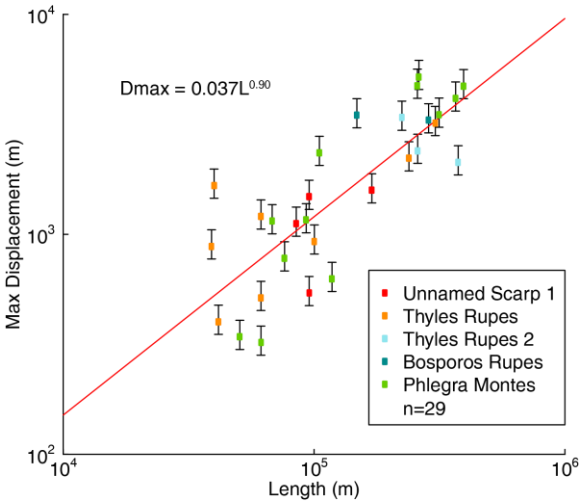

Figure 2) Maximum fault displacement shown as a function of fault length. Regression line is shown in red.

linear least squares regression was performed, closely following the methodology by Clark and Cox [10]. Figure (2) shows the result of this analysis.

Results: Results show that of the 29 faults studied, lengths ranged from 10s to 100s of km with the longest fault measuring 446 km. Maximum fault displacements ranged from 100s to 1000s of m with the highest observed being 5200 m. Two additional fault systems have been mapped but topographic analysis has not yet been included in the regression analysis.

In map view, the faults all appear similar in morphology with linear to curvilinear map traces. Four of the fault zones are considered complex fault systems consisting of more than three individual faults with complex overlap and spacing map patterns. Other faults occur as single, isolated surface-breaking scarps. Faults with minor amounts of superposed craters were preferred for this study so that an adequate number of throw measurements could be taken along the fault.

The displacement distributions generated for each fault or fault system are generally peaked, with the maximum displacement occurring in the center of the mapped fault trace. However, there are some fault systems with peaked general displacement distributions that show individual faults with skewed maximum displacement towards one of the fault tips.

Discussion: The displacement-length regression statistics (Fig. 2) reveal a scaling exponent (c) of c = 0.9. This compares well with the findings by Clark and Cox [10], who find an average scaling exponent of c = 0.946 for 11 evaluated fault data sets. Exponents at or around c = 1 indicate linear scaling relationship between the displacement and length for the faults [e.g., 5, 6, 10]. The scaling exponent may be taken as a measure of whether the studied faults are restricted to a mechanical layer within the Martian lithosphere. If there is a restriction, a power-law function with scaling exponents of $c < 1$ would best describe the data [10]. Unrestricted faults, however, show a linear scaling relationship to the data. Here the data are represented by an exponent of c = 0.9, which is indicative that the faults are not restricted. The peaked displacement distributions further support our finding that the studied faults are not restricted.

Watters et al. [11] and Watters and Robinson [12] had comparable results for displacement-to-length scaling of thrust faults located at the Martian dichotomy boundary. Their displacements ranged from 270 to 2900 m and fault lengths > 400 km were reported (Amenthes Rupes). The faults we studied have somewhat higher displacements of 321 to 5200 m but show a similar length range. Accordingly our results yield a somewhat higher displacement-length ratio, similar to that of terrestrial faults [5, 6].

Conclusions: Mapping and topographic analysis of thrust fault-related landforms in the southern highlands of Mars reveal that they form large mountain ranges that can be in excess of 1000 km in length with up to 3 km of relief. We have identified and studied 6 of these fault zones, with results indicating that fault displacements were as high as 5200 m for a dip angle of 30°, a value exceeding the highest previously reported maximum thrust fault displacement on Mars. Additional large thrust fault-related landforms exist in the southern highlands on Mars. Their inclusion in our analysis will substantially add to the body of knowledge on the dimensions, scaling, and architecture of thrust faults on Mars.

References: [1] Schulz, R. A. et al. (2010) in *Planetary Tectonics*, 457−510. [2] Klimczak, C. (2014) In: Encyclopedia of Planetary Landforms, Springer NY. [3] Schultz, R. A. and Watters T. R. (2001) *Geophys. Res. Let., 28*, 4659−4662. [4] Watters, T. R. (2003) *J. Geophys. Res., 108*, 5054. [5] Cowie, P. A. and Scholz, C. H. (1992) *J. Struc. Geol., 14*, 1149−1156. [6] Dawers, N. H. and Anders, M. H. (1995) *J. Struc. Geol., 17*, 607−614. [7] Kling, C. L. and Klimczak, C. 2015. *LPS, 46*, abstract 1557. [8] http://www.jennessent.com/arcgis/shapes_graphics.html [9] http://www.r-project.org/index.html. [10] Clark, R. M. and Cox, S. J. D. (1996) *J. Struct. Geol., 18*, 147-152. [11] Watters T. R. et al. (2000) *Geophys. Res. Let., 27*, 3659-3662. [12] Watters T. R. and Robinson M. S. (1999) *J. Geophys. Res., 104*, 18,981-18,990.